

### *Supplementary Information*

## Carboxyl functionalized graphene oxide based electrochemical sensor for detection of dopamine in presence of ascorbic acid, uric acid and synthetic cerebrospinal fluid

Priyakshi Bordoloi & Diganta Kumar Das\*

Gauhati University, Department of Chemistry, Jalukbari, Guwahati 781 014, Assam, India

\*E-mail: diganta\_chem@gauhati.ac.in

*Received 10 December 2021; revised and accepted 29 March 2022*

<b>S. No.</b>	<b>Contents</b>	<b>Pg. No.</b>
1	UV-Visible absorption spectroscopy	2
2	FT-IR spectroscopy	2
3	Powder X-ray Diffraction studies	2
4	Thermogravimetric Analysis	2
5	Scanning Electron Microscopic studies	3
6	Fig. S1 — UV-Visible absorbance spectra of (a) aqueous GO dispersion, and (b) aqueous CGO dispersion	3
7	Fig. S2 - FT-IR spectra of (a) GO and (b) CGO, in KBr pellet	3
8	Fig. S3 – Powder X-ray diffractogram of (a) GO and (b) CGO	4
9	Fig. S4 – % Weight loss versus temperature curves obtained from thermogravimetric analyses of (a) GO and (b) CGO	4
10	Fig. S5 – FESEM images of (a) GO and (b) CGO	5

### **UV-Visible absorption spectroscopy:**

The UV-Visible absorption spectrum of GO and CGO shows two peaks. In GO,  $\lambda_{\text{max}}$  peak is observed at 227 nm due to  $\pi \rightarrow \pi^*$  transition of the atomic C-C bonds (conjugation) and a shoulder is observed at 310 nm due to  $n \rightarrow \pi^*$  transition of the carbonyl groups. Similarly, in CGO,  $\lambda_{\text{max}}$  peak is observed at 234 nm ( $\pi \rightarrow \pi^*$  transition of the atomic C-C bonds and carbonyl groups) and a shoulder is observed at 307 nm ( $n \rightarrow \pi^*$  transition of the carbonyl groups) (Fig. S1). Due to the presence of unsaturated carbonyl groups in CGO, the  $\pi \rightarrow \pi^*$  transition requires lesser energy, so it absorbs at a longer wavelength.

### **FT-IR spectroscopy:**

The FT-IR spectrum of GO shows peaks at  $3427 \text{ cm}^{-1}$  (O-H str.),  $2925 \text{ cm}^{-1}$  and  $2850 \text{ cm}^{-1}$  (asymmetric and symmetric str. of  $-\text{CH}_2$ ),  $1594 \text{ cm}^{-1}$  (C=C str.),  $1388 \text{ cm}^{-1}$  (C-O str.),  $678 \text{ cm}^{-1}$  (ar. C-H bending). The FT-IR spectrum of CGO shows peaks at  $3447 \text{ cm}^{-1}$  (O-H str.),  $2926 \text{ cm}^{-1}$  and  $2850 \text{ cm}^{-1}$  (asymmetric and symmetric str. of  $-\text{CH}_2$ ),  $1686 \text{ cm}^{-1}$  (C=O),  $1621 \text{ cm}^{-1}$  (C=C str.),  $1379 \text{ cm}^{-1}$  (C-O str.),  $750 \text{ cm}^{-1}$  (ar. C-H bending) (Fig. S2)

### **Powder X-ray Diffraction studies:**

The powder X-ray diffractogram of GO shows the characteristic peak at  $2\theta = 9.85^\circ$ , corresponding to an interlayer spacing  $d_{\text{avg}} = 8.97 \text{ \AA}$ . This peak is observed for CGO at  $2\theta = 8.88^\circ$ . The interlayer spacing for CGO increases to  $d_{\text{avg}} = 9.95 \text{ \AA}$ , which indicates the presence of bulkier carboxyl groups in place of other oxygen functionalities (Fig. S3). The [002] reflection is attributed to the removal of stacking nature in GO, which is again established in CGO.

### **Thermogravimetric Analysis:**

The thermal decomposition of GO and CGO was studied using TGA. In GO, the weight loss upto  $100^\circ \text{C}$  is due to the removal of water molecules bound to the surface. Major weight loss is observed from about  $200^\circ \text{C}$  to  $270^\circ \text{C}$ , due to the release of carbon monoxide, carbon dioxide and steam from the most labile functional groups. The further slow weight loss from  $300^\circ \text{C}$  is due to the removal of more stable oxygen functionalities. The TGA curve of CGO shows weight loss up to  $100^\circ \text{C}$  due to the release of surface bound water molecules. Further weight loss occurs from about  $200^\circ \text{C}$  due to the removal of all the oxygen functionalities (Fig. S4).

### Scanning Electron Microscopic studies:

The FESEM image of GO shows sheet-like surface morphology. ‘Ripple’ like morphology is observed for CGO, which hints the presence of carboxyl groups in between the ripples (Fig. S5).

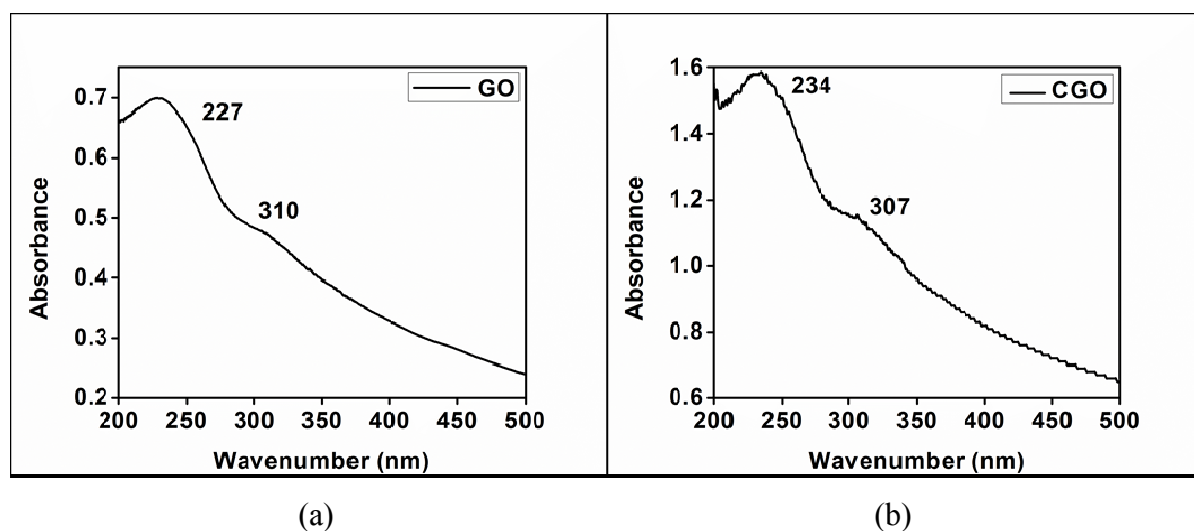


Fig. S1 - UV-Visible absorbance spectra of (a) aqueous GO dispersion, and (b) aqueous CGO dispersion

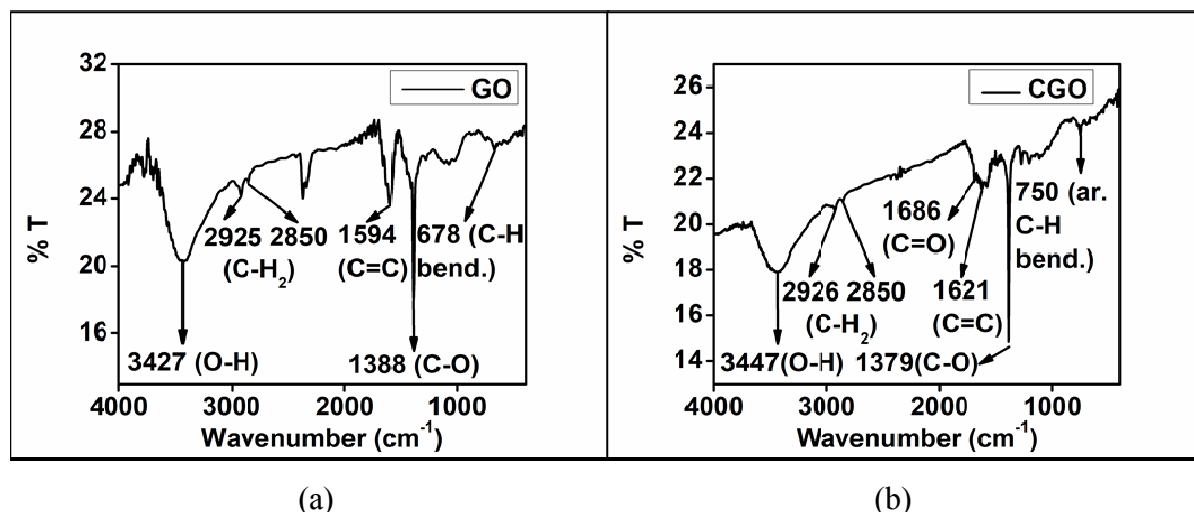
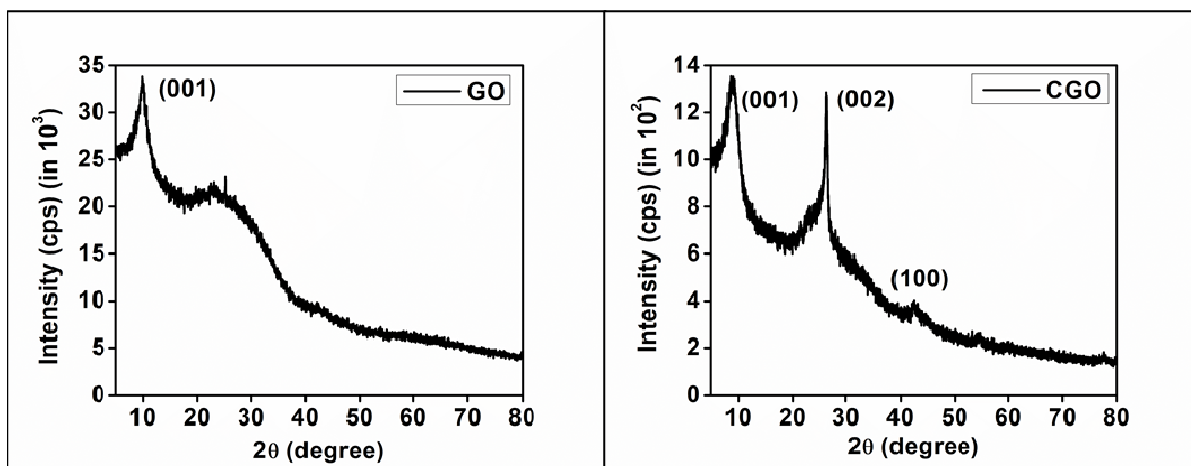


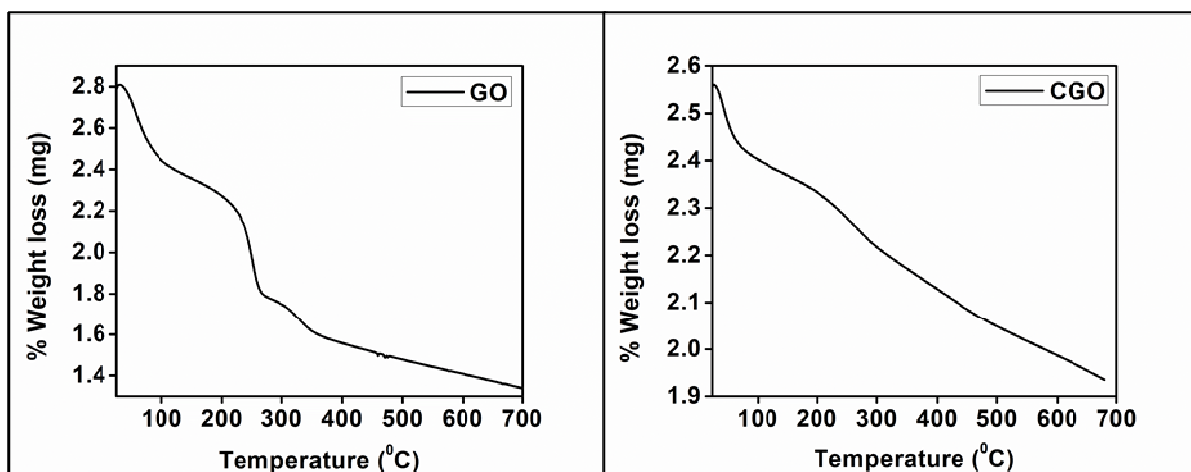
Fig. S2 - FT-IR spectra of (a) GO and (b) CGO, in KBr pellet



(a)

(b)

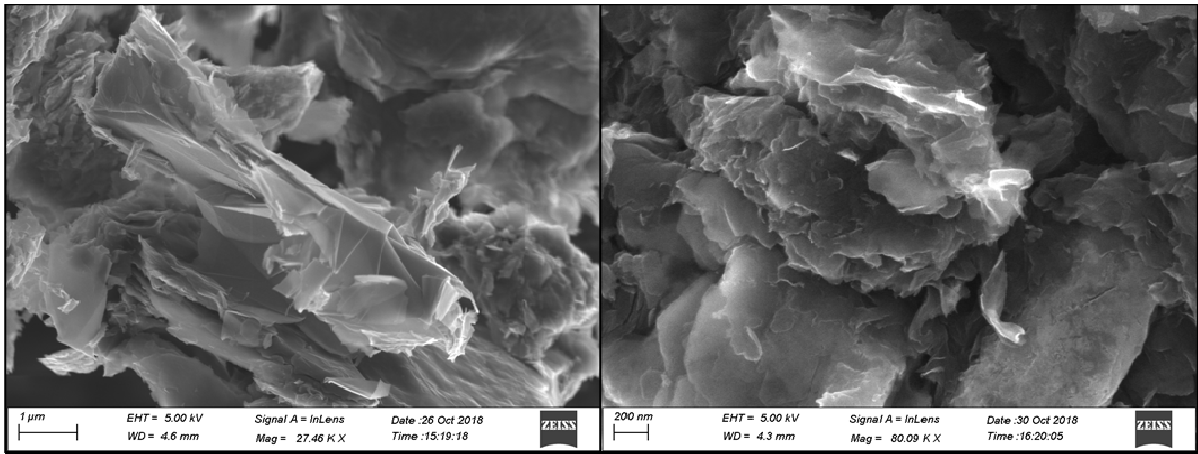
Fig. S3 – Powder X-ray diffractogram of (a) GO and (b) CGO



(a)

(b)

Fig. S4 – % Weight loss versus temperature curves obtained from thermogravimetric analyses of (a) GO and (b) CGO



(a)

(b)

Fig. S5 – FESEM images of (a) GO and (b) CGO